

Investigations Into the General Fusion Company

Reactor Concept

Prepared by:

Maximilian Mendoza, Daniel Zhan

Sibley School of Mechanical and Aerospace Engineering

Cornell University, Ithaca, NY, USA

May 16th, 2022

I. Introduction to General Fusion and Fusion in General

A. Introduction to Fusion in General

A growth in the general interest in fusion reactor concepts and global climate change have caused rapid development of these devices in both the public and private sector. New interest, mainly centered in North America, has given rise to 20 private fusion companies [2]. With the International Atomic Energy Agency's (IAEA) fusion reactor design classification, it can be seen that the private sector is where many of the innovative, yet risky/unproven designs tend to fall [2]. This is the case for the company of interest within this report – General Fusion.

Fusion can be generalized into three main methods: magnetic confinement fusion (MCF), inertial confinement fusion (ICF), and magneto-inertial fusion (MIF). These spaces are defined by the relative density of the fusion plasma. MCF reactors have low density plasmas that achieve high temperatures, while ICF reactors have high density plasmas at lower temperatures [2]. MIF reactors span the spaces in between the MCF and ICF extremes, implementing a middle ground in an attempt to mitigate the drawbacks of the two methods individually. All three of these methods seek to achieve a fusion gain (Q_{fus}) value that is greater than one. This value is dependent on the fusion triple product, which is the product of the plasma temperature, density, and confinement time. The values in this triple product differ between the fusion methods mentioned above. MCF reactors use magnetic fields to confine and manipulate the fusion reactions in a long-pulse plasma (steady state) [2]. These plasmas are low density, so they require a much longer confinement time and substantial added heating in order to reach fusion triple product conditions. ICF reactors generate an extremely high plasma density and temperature, but this process occurs in a very short confinement time. This means this method must be pulsed in order to reach viable fusion conditions. MIF reactors combine the methods of the previous two to

reach fusion triple product conditions. When compared to MCF reactors, they have a high plasma density and relatively short confinement times (not as short as ICF reactors, though). This medium density plasma is then compressed even further by a driver (as seen in ICF reactors) to reach the necessary conditions [2]. A diagram comparing these three reactor configuration paradigms is shown below in figure I.A.1.

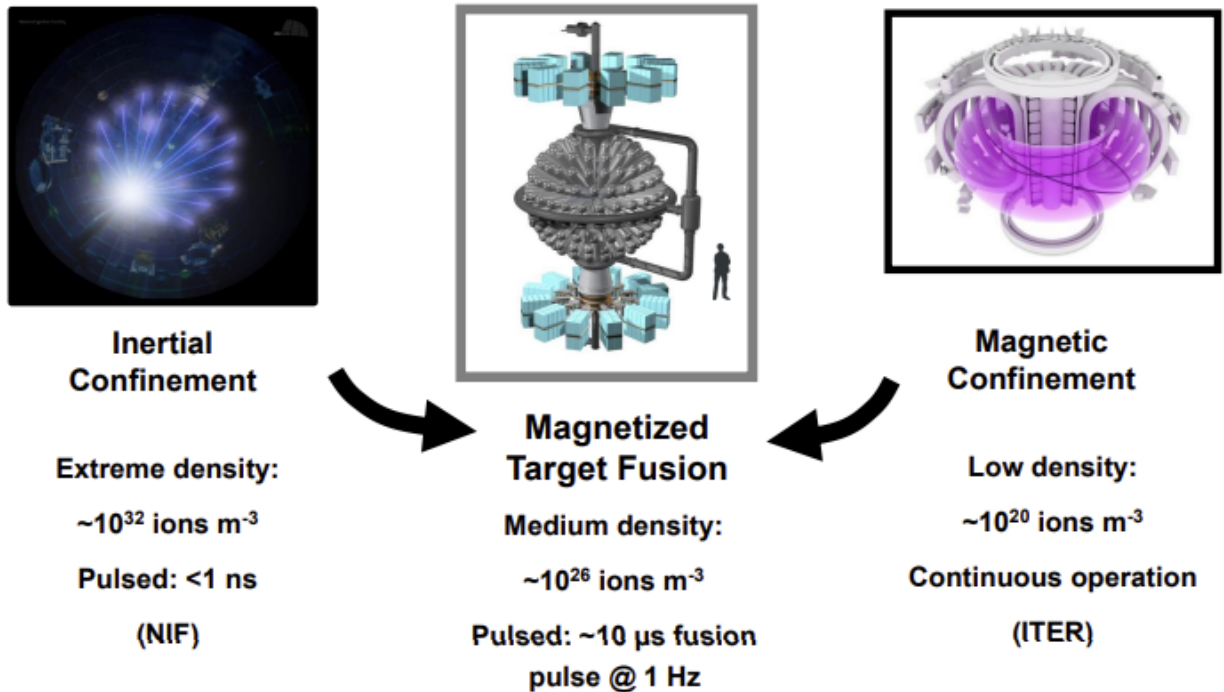


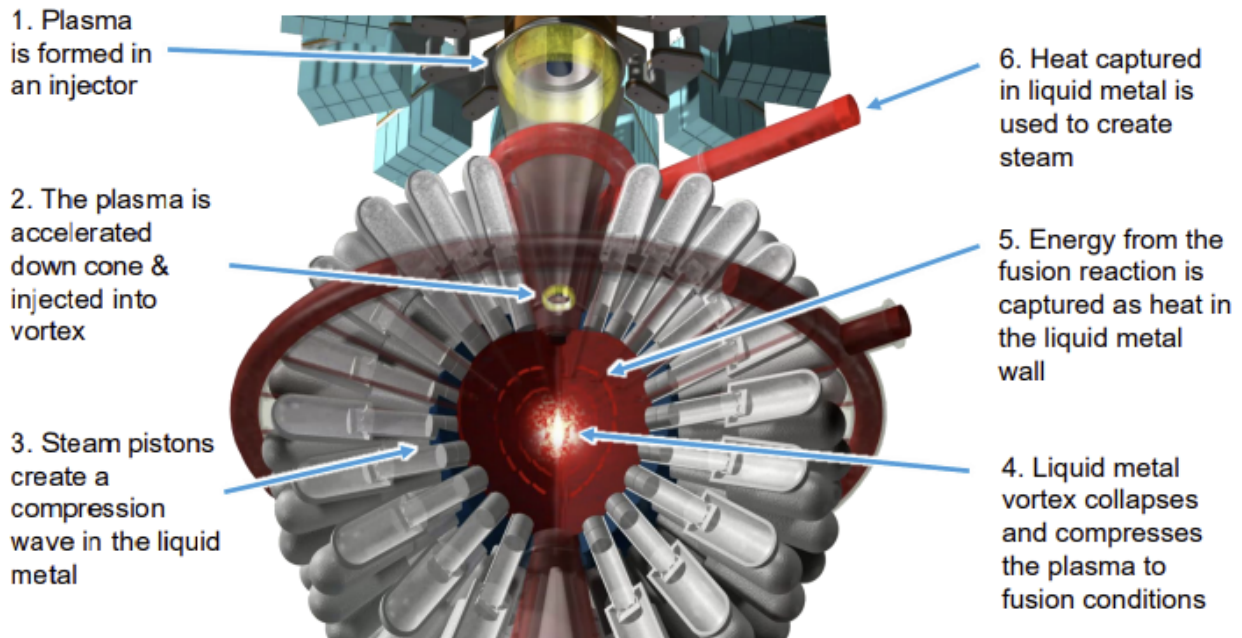
Figure I.A.1. This diagram compares various reactor configuration paradigms. Source: [9].

B. Introduction to General Fusion

General Fusion is a Canadian company that is working towards a commercially viable fusion power plant, with an emphasis on using technologies that are well-researched and established in order to build a working prototype plant quickly. Their approach to fusion, named “Magnetized Target Fusion” (MTF), a sub-category of the MIF reactors described in the above section, is considered a relatively low-cost path to viable fusion. Their “Fusion Demonstration Plant”, which is a 70% scale model of their intended fusion reactor, is set to begin operations in

2027, and they have received \$430M in funding from a variety of private and government investors as of 2021.

The prototypal fusion reactor design itself contains a few elements common to many other fusion reactors and a few fairly unique design choices. A visual of the reactor prototype can be seen in figure I.B.1. The exterior of the fusion facing chamber is a spherical steel shell surrounded by pneumatic pistons in an approximately symmetric configuration. A flowing liquid metal “inner wall” is pumped tangentially into the sphere equator, where it protects the steel shell from high-energy particles (especially neutrons) and heats up upon facing the deuterium-tritium (DT) fusion reaction, then drains out the bottom into heat exchangers to export energy from the reaction. Two plasma injectors facing each other inject DT compact toroids (CTs) into the chamber - upon contact these CTs merge into one DT spheromak configuration. The external pistons simultaneously strike the liquid metal wall to send a shockwave through it, thereby compressing the spheromak fuel into a plasma fuel that reaches fusion conditions for a time on the order of microseconds, whose fusion products then emerge with an increased kinetic energy and heat up the liquid metal wall. These fusion reactor elements are the main focus of this research project and will be covered in greater detail in the rest of this paper.



*The sphere is filled with liquid **Lead-Lithium** metal. The liquid metal is pumped tangentially at the equator so that it spins and creates a vortex.*

Figure I.B.1. This diagram of the reactor prototype describes the order in which reactor processes occur. Source: [13].

II. General Fusion's Approach

A. Plasma Injectors

Looking at one of the central elements of generating fusion energy, a brief overview of General Fusion's plasma confinement method into a spheromak configuration is given.

The plasma structure of the central vacuum consists of self-contained plasma rings known as compact toroids, which merge to form a single ring in the compression region. The merging takes place in the "evacuated volume of a free-surface cortex in the center of a rotating flow of liquid metal" [4]. The rotation is thought to mitigate sources of error and instability listed in section IV, and can be seen in the overall reactor scheme in figure I.B.1 above. There are two

primary devices that General Fusion are using for the plasma: a small direct formation testing apparatus called a Magnetized Ring Test (MRT) and a set of larger conical plasma injection devices (PI-1 and PI-2) (seen in figure II.A.1) [4]. Both of these instruments use a magnetized Marshall gun to achieve the spheroid configuration in the central cavity. These devices work by accelerating the CT via generating an unbalanced toroidal flux, which is created by an external railgun current that passes along the back radius of the CT. The magnetic pressure from this flux

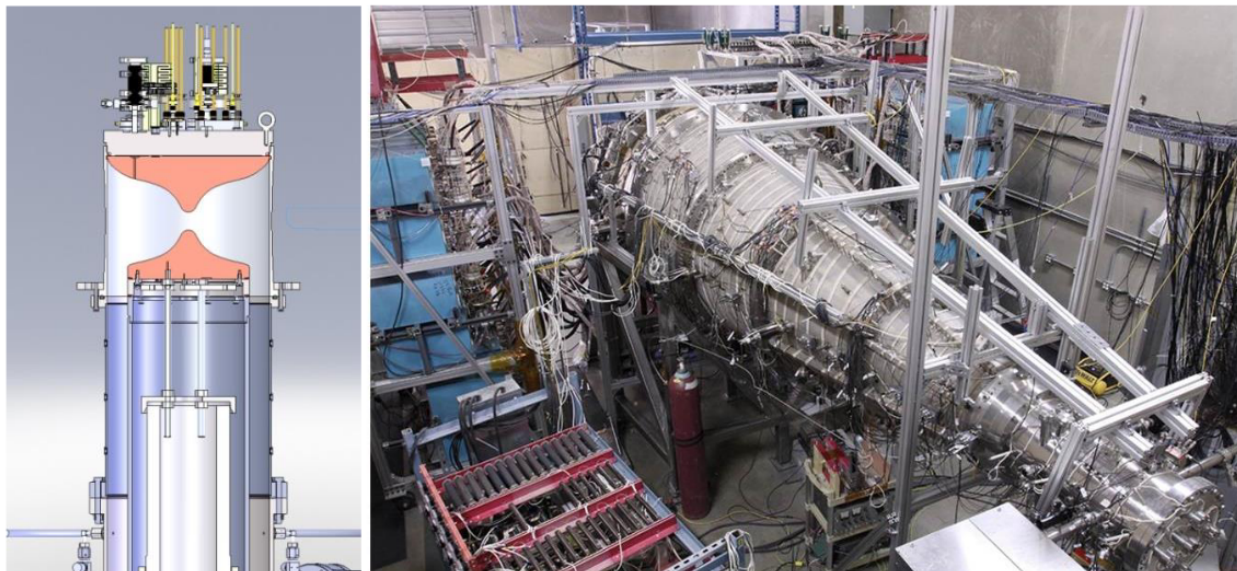


Figure II.A.1. (a) Magnetized Ring Test (MRT) on left, (b) Plasma Injector-1, right. Source: [4].

accelerates the CT to speeds faster than 100 km/s, and this provides the force to compress the two CTs together into conical self-similar electrodes with a 4x compression ratio [4]. The MTF configuration would have the plasma injectors (PI-1 and PI-2) positioned opposite each other on the sphere, as seen later in figure II.B.1. The directional entry from both sides would allow the net momentum of the final converged spheroid to be zero and allow for the pressure wave to apply uniformly. Alternatively, they have considered only having one CT, which may have advantages if practical fusion conditions can be reached with it [4].

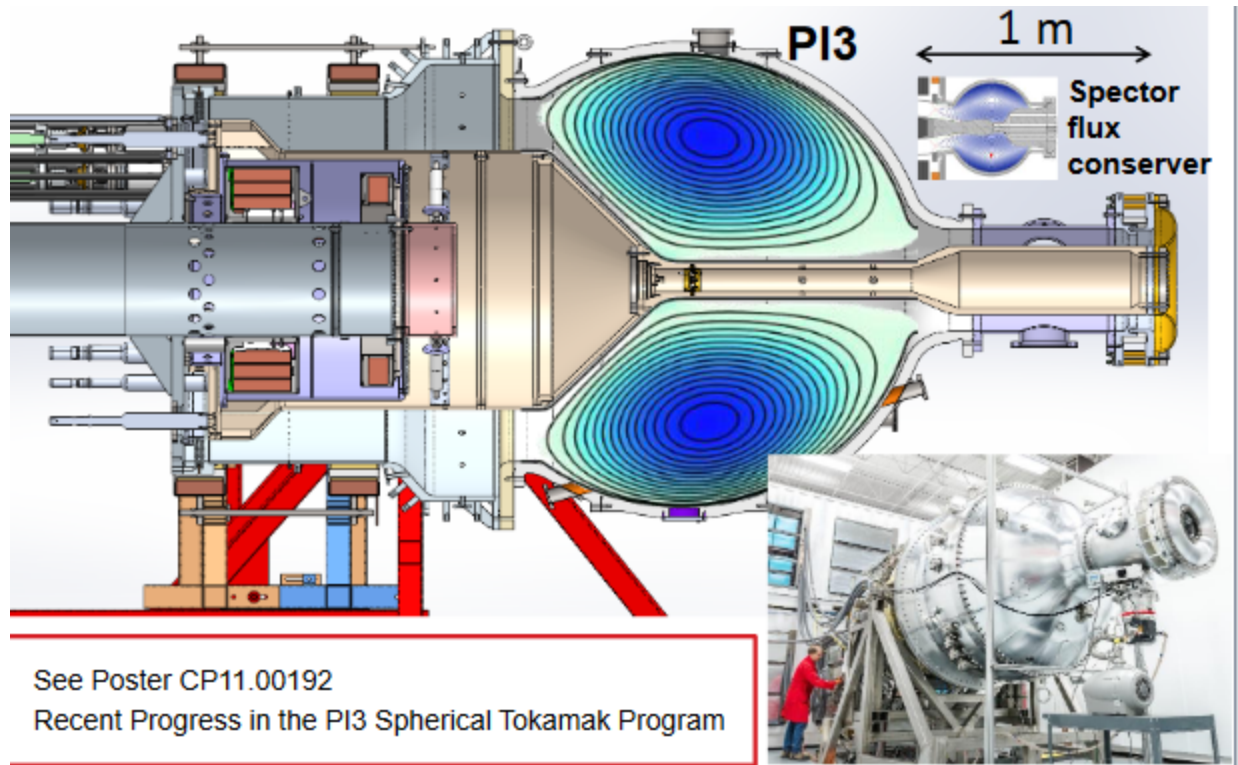


Figure II.A.2. General Fusion's newest large injector, PI3, is designed to demonstrate formation of a spherical tokamak target suitable for use in our large scale magnetized target fusion prototype. Source: [9].

Looking at the results from the plasma compression, when the plasma reached 4x radial compression, the electron temperature was far below the expected value for adiabatic conditions. The importance of the adiabatic compression condition is explained more thoroughly in section II.C. General fusion is still looking into possible reasons for why this might be the case. One possibility is that there is enhanced transport via magnetic fluctuations and/or the high levels of visible, UV, and soft X-rays, which add uncertainty into the system [4]. Another challenge that results with this form of plasma compression is the high plasma beta values, which was found to be around 0.32 at maximum (see figure II.B.2). The smaller MRT device actually tries to form the high flux CT directly within the aluminum liner, completely skipping the acceleration and

pre-compression stage issues with PI-1 and PI-2. MRT devices are also known for their high beta stability and are thus good for testing CT formation into a spheromak shape [4].

For future development of the plasma injector process, General Fusion seeks to keep working with high efficiency plasma injectors that are able to operate at the high powers required for fusion. They have even begun development on an alternative design (PI-3) seen in figure II.A.2, which uses more of a trumpet shape in order to minimize the errors and problems stated in the previous paragraph.

B. Liquid Metal Wall

Fusion reactor prototypes require a plasma-facing component that achieves the following goals: the fusion “blanket” must 1) protect other reactor components and human operators from incident radiation, 2) extract energy from the fusion reaction, 3) keep the plasma free from impurities, and 4) breed tritium for use in the DT fusion reaction. One popular concept for a fusion blanket that satisfies these requirements in an Inertial Confinement Fusion configuration is the “liquid metal wall” (LMW). In this section of the paper, we will discuss the design decisions of General Fusion’s LMW and how it satisfies General Fusion’s reactor requirements.

Figure II.B.1. is a general diagram of the reactor prototype. As indicated by the orange sections of the diagram, the LMW is pumped in using injectors (conventional liquid pumps) tangentially into the equator of the spherical vessel and forms a cylindrical vortex for the plasma fuel to occupy and react, is heated up upon absorbing the kinetic energy of incident neutrons emerging from the fusion reaction, and then exits the vessel through the top and bottom into a turbine generator to export energy from the fusion chamber. Once cooled, the LMW is pumped back into the vessel to resume the cycle.

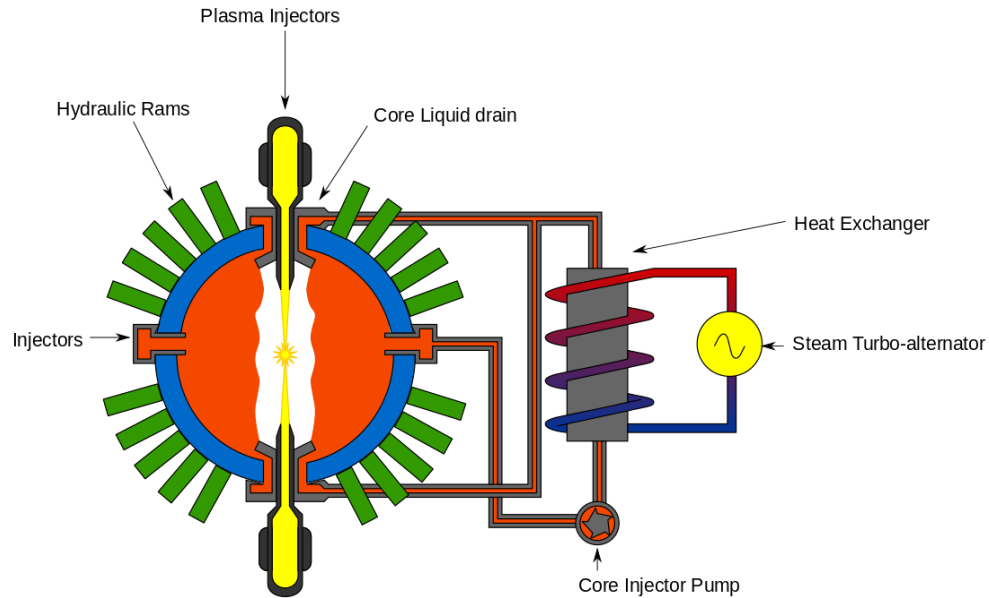
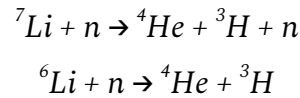


Figure II.B.1. General Diagram displaying various functionalities in the reactor prototype, with an emphasis on LMW flow. Source: [1].

The LMW itself is a molten (liquid) Lead-Lithium Eutectic composed of 83% (by atom count) Pb and 17% Li. This alloy was chosen for numerous reasons, including the fact that it has a low melting point, which allows for easy startup and pumping even when the fusion chamber is still cold [10]. Additionally, the liquid has a low vapor pressure, and its high inertial mass allows it to keep the plasma compressed for longer. The steel pistons, which provide the shockwaves necessary to inertially confine the fuel into the density necessary for fusion, have a similar acoustic impedance to lead (a phenomenon discussed in detail in the next section, II.C), which allow energy in the shockwaves to pass through rather than trapping energy at the interface between the LMW and pistons and in the LMW itself [10]. Lastly, the lithium in the mixture at the percentage indicated allows for a sufficient ratio of tritium breeding - the incoming high energy neutrons out of the fusion reaction react with lithium atoms to produce tritium, which are then chemically extracted for use in later fusion reactions.

The LMW protects reactor components and operators from resultant radiation from the fusion process primarily by reducing neutronic flux on reactor structures and lowering the energy of neutrons that do manage to emerge. Additionally, the incident neutrons react with the lithium in the blanket to produce tritium to be used in later fusion reactions. This process happens via two possible reactions:



These reactions result in a tritium breeding ratio of between 1.6 and 1.8; the ratio is greater than 1 due to the extra neutron that is produced in the first reaction, which can then initiate another tritium breeding reaction. This blanket is necessarily thick to reduce the number of neutrons that escape and damage the reactor's insides, but making the blanket too thick results in the overproduction of tritium, so an optimal liner thickness is necessary to achieve both conditions. As a result of the constantly flowing liner, any impurities resulting from the fusion reaction are swept out of the reaction chamber; sputtering of the steel vessel into the fusion fuel is also mitigated significantly by the absorption of neutrons into the liner, thereby keeping the fusion fuel relatively free of impurities.

One condition imposed upon General Fusion's LMW that isn't present in typical ICF configurations is that the inertial confinement occurs via piston-generated shockwaves that have to propagate through the LMW before reaching and compressing the plasma. Lead was chosen as the primary component in the LMW for this reason as discussed before - a similar acoustic impedance between steel and lead allows the steel pistons to transfer energy through the lead LMW without much loss of energy in the liner. The drastically different acoustic impedance between the LMW and the internal vacuum surrounding the plasma causes these shockwaves to nearly completely reflect back into the liner, generating the maximum possible momentum to

compress the plasma. A few instabilities and other challenges may arise from the non-uniform nature of finite pistons striking the LMW to compress the fusion plasma - these will be discussed in Section IV.

Another difference between ICF and General Fusion's approach are the magnetic fields present in MTF. The LMW is a conductor, which may result in unexpected MHD effects in the liner that need to be mitigated. This is discussed in Section IV as well.

C. Gas Piston Compression

A final important element of General Fusion's approach is the acoustically driven compression of the MTF concept. This makes use of modern servo controllers to synchronize piston impacts on the reactor itself that creates a large amplitude acoustic wave that propagates through the liquid metal liner [4].

Before getting into the experiment and simulation data that General Fusion has provided over numerous testing cycles and prototypes, a theoretical framework for adiabatic compression of Deuterium gas was performed by David W. Kraft, which gives a general overview of this method's potential. Using the framework of rapid, adiabatic compression by a piston in an insulated chamber, the reduction in the degrees of freedom of the gas and exploitation of the fuel density (N^2) factor in generating fusion power both lead to "appreciable fusion rates at lower temperatures" [3]. This is important because lower temperatures means less stress on the system and its components as fusion conditions are reached. By treating Deuterium as an ideal gas, equation II.C.1 below can be derived by equating the temperature rise to a compression ratio (β) and the degrees of freedom of the gas (f):

$$T = T_0 \beta^{\frac{2}{f}}. \quad (\text{II.C.1})$$

From the relation, it can be seen that if gas particles are confined (lower degrees of freedom) and compressed, a larger temperature rise is achieved from a given energy input [3]. Looking at the fusion rates for an ideal gas, it was shown that temperatures, reaction rates, and the ratio of fusion power produced to work needed to compress the piston ($\delta E/W$) increase with higher compression ratios and lower degrees of freedom. With an f of 1 and a β of 200, it was shown that the fusion power produced exceeded the work needed to compress the piston. Moving past the ideal gas assumption and moving into a more realistic van der Waals model of the gas, the highest $\delta E/W$ at the same compression ratio/degrees of freedom is around 300 times greater than that of the ideal gas (from 14 for the ideal gas to 4100 for van der Waals). Thus, even a perfect gas assumption underestimates the efficacy of the compression model [3]. If the chamber is nearly perfectly insulated, the energy released (from nuclear processes or radiation from charged plasma particles) and the work to compress the plasma directly goes back into the system which increases the thermal energy and fusion reaction rates further [3].

Although the results of the Kraft model of gas compression are promising, it does make a fair number of assumptions that impact how it may be implemented in reality. Firstly, it assumed that all energy released by the explosive charge was used to drive the piston and that there were no frictional losses involved in the transfer. Also, this model does not account for the losses from the energy used to establish an electric discharge and magnetic fields required to reduce the degrees of freedom of the fuel. Second, this model ignored the volume compression and temperature rise associated with the pinch effect as well as shielding effects from the electron gas, which serve to increase the probability that fusion occurs. Finally, this model assumed that fusion only occurred at the moment of maximum compression, which underestimates the real case

where fusion can happen with the release of energy during the compression process, which is continuous [3].

Building off of this modeling, General Fusion has developed a bridge to the actual solution - a prototype called the Mini-Sphere. As seen in figure II.C.1, it consists of 14 pistons arranged on a steel sphere with an inner radius of 0.5 m. The pistons work in three parts,

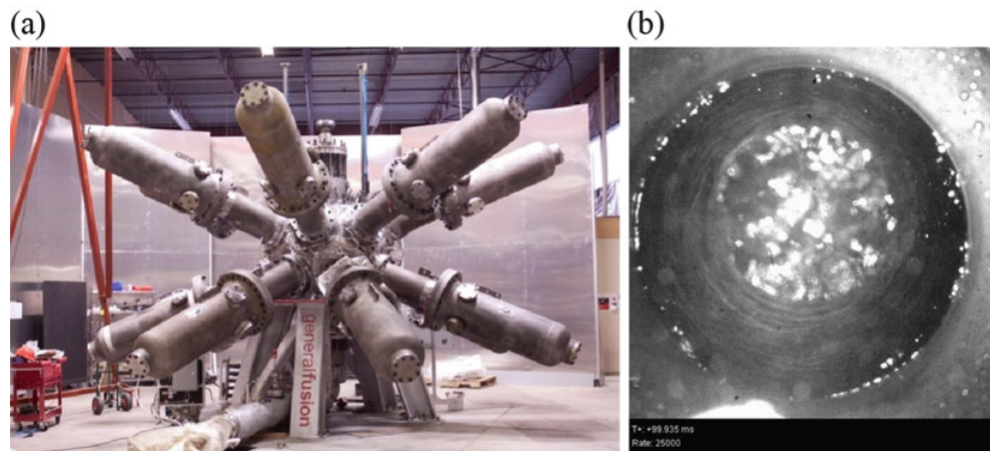


Figure II.C.1. On the left is the Mini-sphere compression system at General Fusion Inc. (a) and a top down view of the liquid lead vortex inside the compression system (b). Source: [1].

highlighted by the CAD image in figure II.C.2. The system consists of three parts: a 100 kg hammer piston (seen in red), a floating anvil piston (seen in green), and liquid lead tank (seen in blue) [1]. The hammer piston strikes the floating anvil at speeds around 50 m/s from the compressed gas, which in turn propagates a pressure wave that reaches the interface between the steel and liquid lead. Once the wave propagates to the center and converges due to the symmetrical geometry, it hits the vacuum-lead interface, which almost entirely reflects the wave due to differences in acoustic impedances. This is the interaction that causes a rapid acceleration inward in the cavity and the high compression ratios needed to achieve fusion conditions.

Acoustic impedances are material properties that are defined by equation II.C.2, which are dependent on the density of the material (ρ) and the speed of sound through the material (c)

$$Z = \rho c. \quad (\text{II.C.2})$$

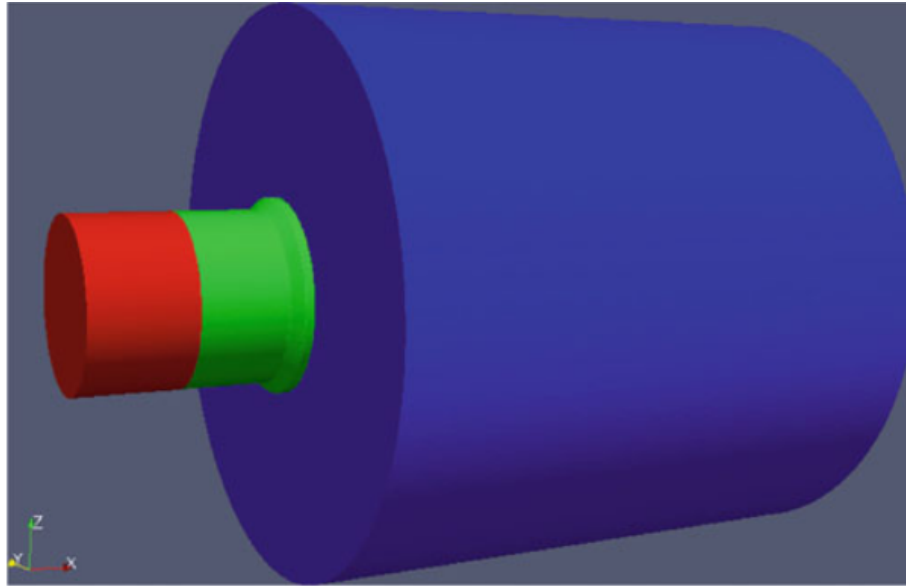


Figure II.C.2. Three-body system (hammer (red), anvil (green), and lead tank (blue)) simulated with Y code to obtain temporal and spatial structure of the pressure wave transferred by the anvil piston into molten lead. Source: [1].

This relation dictates the energy transmitted/reflected from one material to another, which is steel/lead in General Fusion's case. The closer the Z values of the two materials, the more energy gets transmitted between them [1]. General fusion simulated three different materials for the lead tank: steel, solid lead, and liquid lead. The last of those cases being the closest to the real situation where the anvil piston would be impacting the molten lead that forms the liquid metal wall. With use of openFOAM software, the team at general fusion were able to get numbers for the propagation and convergence of the pressure wave, as seen in figure II.C.3. As seen in the image in part (d) of the figure, at the convergence of the waves reaches a maximum pressure of 150 Megapascals on the order of microseconds.

Looking at the numbers and economics for the pneumatic piston approach, the 100 MJ acoustic pulse range can be achieved for a relatively cheap price of around \$0.2 per J, while the more pervasive alternative of high voltage pulsed power for electromagnetic pressure implosion is around \$2 per J (an order of magnitude more expensive). Also, for a fully efficient reactor, the working gas on the high pressure side of the heat exchange system could even be diverted directly to drive the piston array for compression, which skips over any electrical losses that come with storing energy in a capacitor bank [4]. These along with the preciseness of using the synchronized servos illustrate the vast potential for this method of compression for reaching optimal fusion conditions.

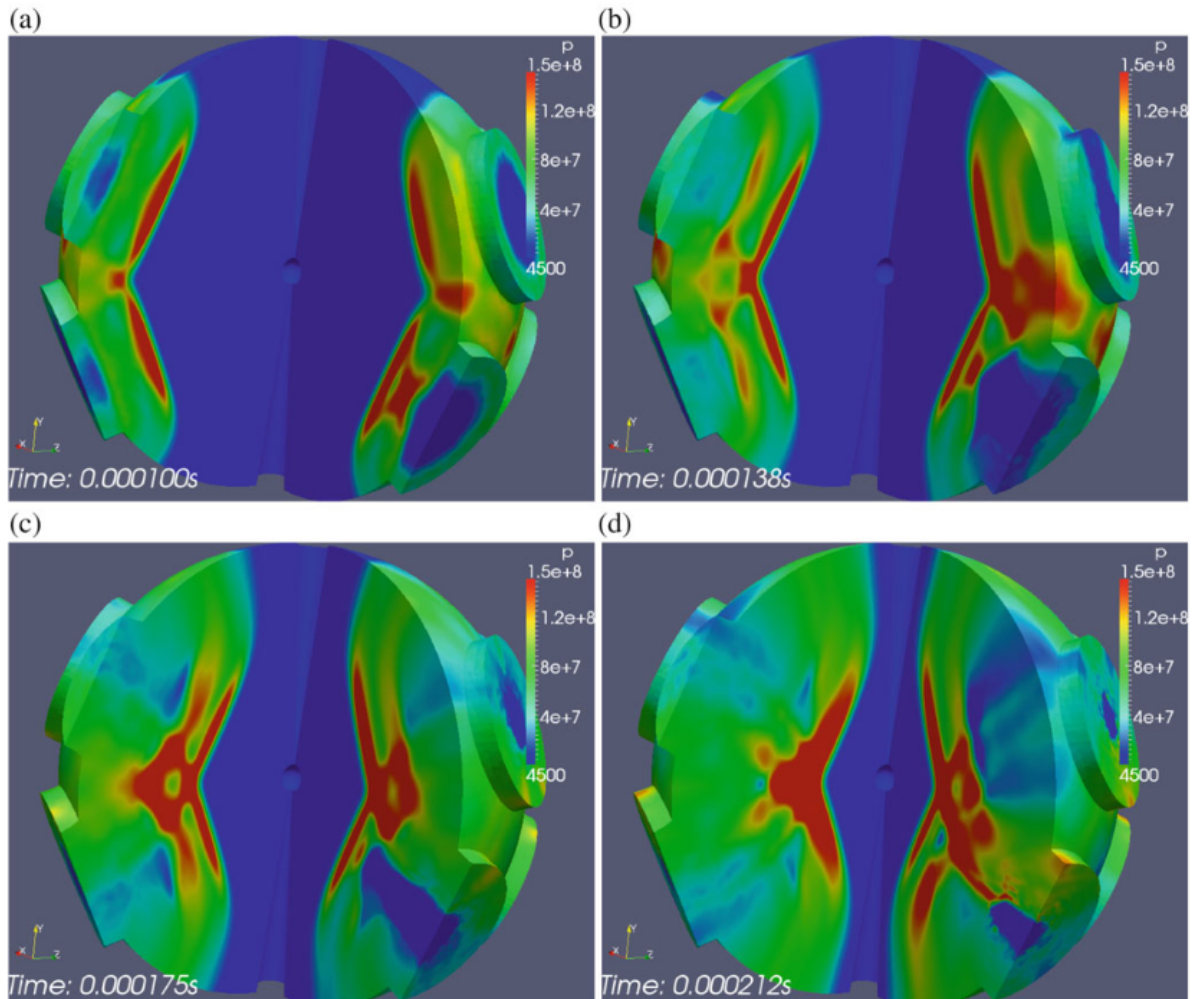


Figure II.C.3. Structure of the pressure wave produced by the fourteen pistons inside current compression system prototype as it propagates through the molten lead obtained with open FOAM (a) $t = 100\mu\text{s}$; (b) $t = 138\mu\text{s}$; (c) $t = 175\mu\text{s}$; (d) $t = 212\mu\text{s}$. Source: [1].

III. Proof of Concept

For any economically viable fusion reactor, the output energy must exceed the input energy. We can work with this requirement to derive a number of general physical requirements that the fusion reactor must meet in order to produce energy.

The Lawson Criterion is a measure of whether or not a fusion reactor can produce more energy in its fusion reaction than it spends in the process. Because a fusion reaction's energy

output correlates with both the peak ion density of the fusion fuel and the time spent at or near this peak ion density, the Lawson Criterion generally states that the product of ion density and confinement time ($N\tau$) exceed some function of ion temperature and other parameters specific to the reactor type. An example of a Lawson Criterion is given in figure III.1 for MCF configurations, which states that $N\tau$ must exceed a function of various energy transfer efficiencies, expected bremsstrahlung radiation, and various other parameters. Because a specific Lawson Criterion has not been published for this particular reactor, we will compare the optimal reactor conditions expected in simulations to a commonly quoted figure that the $N\tau$ value must exceed, found in figure III.2 [14].

$$N\tau_{E^*} > \frac{3(1 - \eta_{in} \eta_{out})T}{\eta_{in} \eta_{out} \frac{\langle \sigma v \rangle_{ab}(T) Q_{ab}}{4(1 + \delta_{ab})} - (1 - \eta_{in} \eta_{out}) A_{br} \sqrt{T}}$$

Figure III.1. The Lawson Criterion in equation form for MCF configurations. Source: [12]

$$n\tau \geq 10^{14} \text{ s/cm}^3$$

Figure III.2. A widely quoted Lawson Criterion figure for DT reactions. Source: [14]

As a general rule, MTF typically satisfies the Lawson Criterion by operating in an intermediate regime between the more extreme regimes of ICF and MCF (as discussed in section I) - it possesses a longer confinement time than that of ICF and a higher achieved density than that of MCF, but has a shorter confinement time than typical MCF configurations and a lower density than typical ICF configurations. Using the theory and prototype of the acoustic compression system, General Fusion provides a model of the ideal scenario of their process. Hundreds of pistons are synchronized via modern servo technology to reduce the volume by three orders of magnitude, the plasma density will be raised from 10^{22} ions/m³ to 6×10^{25} ions/m³,

the temperature from 0.1 keV to 15 keV, and the magnetic field from 5 Tesla to 1600 Tesla. The fusion energy will be generated in the 130 μ s that the plasma is in its maximally compressed state [4]. Another factor of importance is that the confinement time of the plasma is much longer than this compression time so that the compression heating of the plasma is approximately adiabatic (for reasons discussed in [3] and section II.C). To get some numbers for the potential of their compression system, General Fusion ran a one-dimensional Lagrangian spherically symmetric collapse of the Pb liner to the point plasma model. In this example, they sent a 2 Gigapascal acoustic pulse at an outer radius of 1.5 meters. At the plasma-liner interface, the pressure was 12 Gigapascals and it compressed the plasma for 130 μ s by a radial factor of 18. A summary of the plasma parameters is given in figure III.3, where the peak fusion power is 3.6 Terawatts and peak plasma beta is 0.32. The initial conditions are all presently achievable physically, barring the initial magnetic field value (B_0) of 5 Tesla, which is greater than their previous results but not impossible to reach [4].

With a stated confinement time of 130 μ s and an ion density of 6×10^{25} ions/m³, the $N\tau$ product is then 7.8×10^{21} s/m³, or 7.8×10^{15} s/cm³. This exceeds the stated Lawson Criterion minimum of 10^{14} s/cm³ by almost two orders of magnitude, which gives us room for sub-optimal reactor conditions to potentially still satisfy the Lawson Criterion and output more energy than it requires to function.

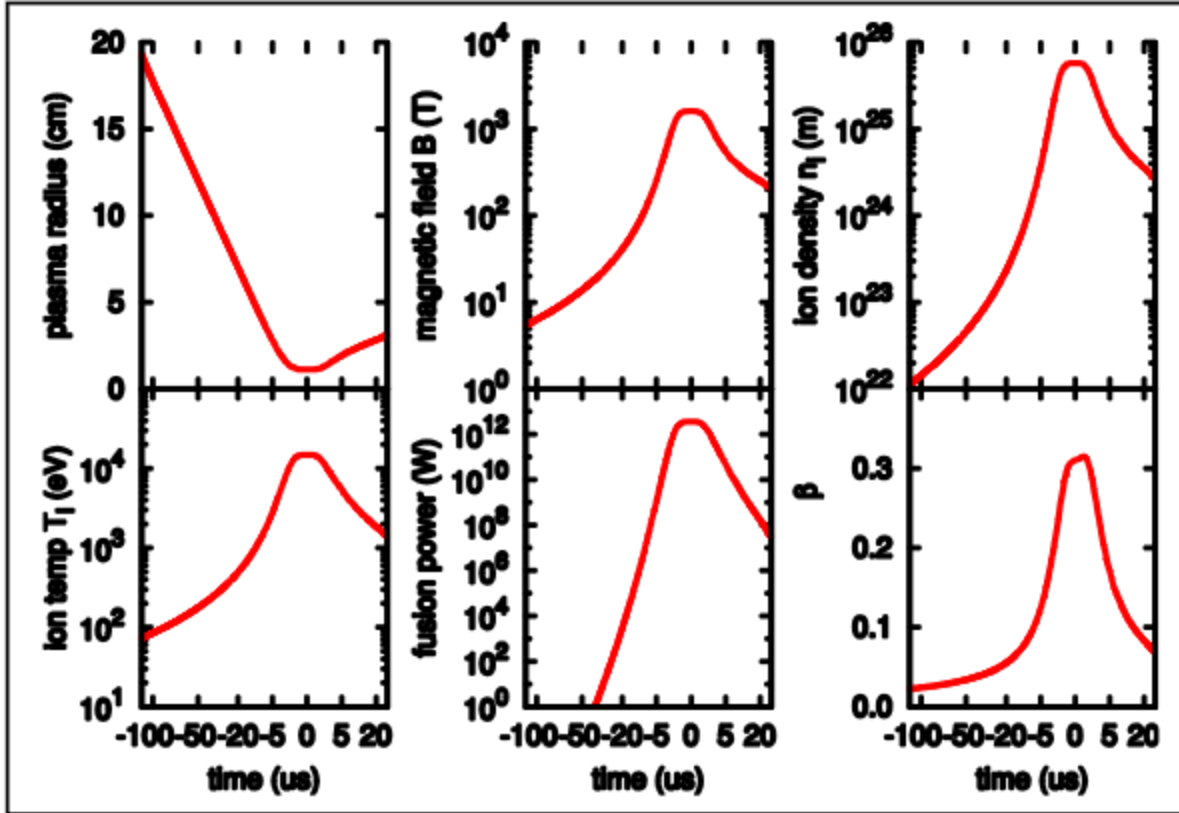


Figure III.3. Time-evolution of plasma parameters in a 1D Lagrangian model of Pb liner coupled to point-plasma model, showing Plasma-liner radius, CT magnetic field, ion density and temperature, fusion power, and plasma beta. Source: [4].

IV. Challenges

A. Challenges with the liquid metal wall

As mentioned briefly at the end of Section II.B (Liquid Metal Wall), unintended MHD (magnetohydrodynamics: the study of the dynamics of electrically conducting fluids) effects will occur when a conducting LMW rapidly converges upon a DT spheromak whose current generates a magnetic field. An illustration of this is shown below in figure IV.A.1 - as can be seen, the rapidly compressed liner absorbs magnetic flux as it converges upon the plasma. 2D MHD simulations show that approximately 30% of the poloidal flux soaks into the wall upon

compression. The advective nature of the poloidal flux field causes the flux to spread throughout the liner when it converges, as can be seen in the red magnetic field lines widening throughout the plasma in the right half of the diagram. Figure IV.A.2 quantifies the amount of flux that enters the liner in MHD simulations.

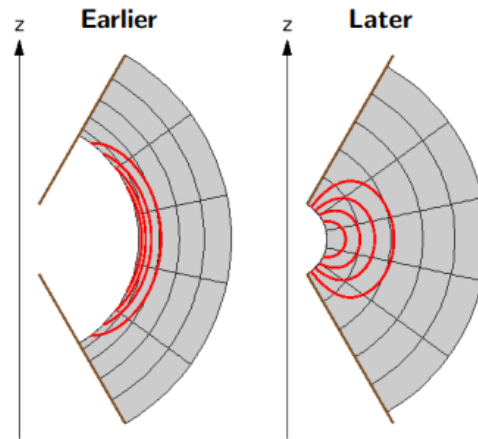
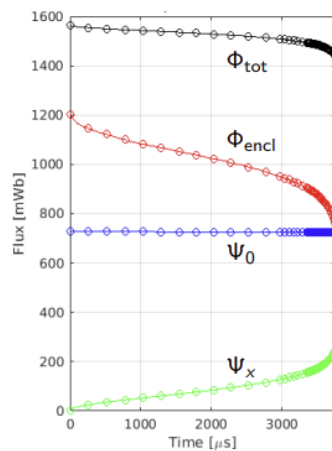


Figure IV.A.1. Time-evolution of magnetic flux through LMW liner. The red lines are magnetic field lines and the gray represents the LMW, which noticeably compresses inwards in the diagram to the right, which causes this magnetic flux to pass through the LMW. Source: [5].

Magnetic fluxes versus time during compression



Poloidal flux, in webers, $\Psi(r, z) \equiv 2\pi\psi(r, z)$

- ▶ **Blue:** $\Psi_0(t)$ is poloidal flux linked by magnetic axis, nearly constant due to good plasma conductivity
- ▶ **Green:** $\Psi_x(t)$, poloidal flux linked by separatrix (i.e., soaked into the liner)
- ▶ Poloidal flux enclosed in the plasma is $\Psi_0 - \Psi_x$

Toroidal flux $\Phi \equiv \int B_\phi(r, z) dr dz$

- ▶ **Black:** toroidal flux $\Phi_{tot}(t)$ in the entire plasma domain
- ▶ **Red:** toroidal flux $\Phi_{encl}(t)$ enclosed by the separatrix

Figure IV.A.2. Time evolution of various components of magnetic flux present in the plasma and liner. Note the amount of flux entering the liner over time, as shown in green. Source: [5].

The loss of current and magnetic flux into the LMW may enhance interaction between the plasma and the LMW, which could increase wall sputtering into the plasma or cool down the plasma and slow the rate of fusion. More comprehensive simulations (including adding in the necessary third dimension) are necessary to definitively understand how to mitigate MHD effects in the liner.

B. Challenges with gas piston compression

Even though the acoustic compression concept is much cheaper and more efficient in some ways compared to other compression methods used in ICF, there are several problems that arise from this method.

First of all, there are a number of instabilities that can affect the uniformity of this pulse, which is itself an issue if it does not happen to be completely uniform. The Richtmyer-Meshkov (RM) instability, which is from accelerating fluids of different densities, could undermine the entire operation of the liquid lead liner compressing the plasma. However, all recent studies and simulations of this instability have been for planar or cylindrical interfaces, not the elliptical one employed here (see figure II.C.3 [d]) [4]. The ability to accurately predict how this effect will manifest in the product is an area of active research for MTF reactors, and could develop to be one of the main limiting factors due to the importance of the uniformity of the pulse. As seen below, asymmetry in the pulse can propagate and non-linearly increase in magnitude (figure IV.B.1).

The material conditions of the materials in this process also limit its potential in certain areas. The most apparent being that of the acoustic impedance mismatch as described in section

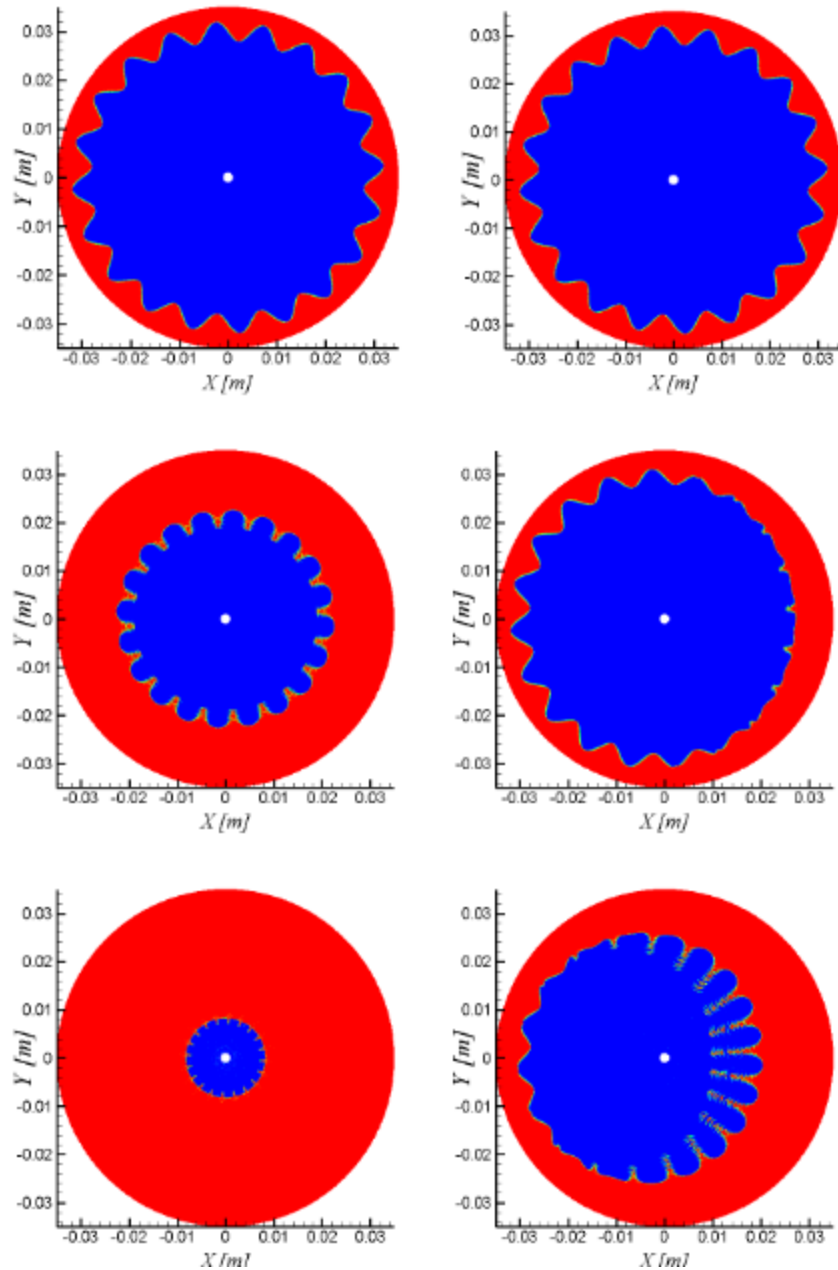


Figure IV.B.1. Effect of the asymmetry of the imploding wave. Left column shows collapse of the initially perturbed air cavity by a perfectly symmetric imploding cylindrical pressure wave. Right column shows collapse of exactly the same cavity when the pressure wave is generated by a single piston (pressure wave arrives from the right).

II.C, which limits the amount of energy transfer from the anvil piston and the molten lead. This also introduces the constraint where they must operate at elevated temperatures when compared to the hammer pistons. On the other hand, even though they do not operate at the heightened temperatures of the anvil, the hammer pistons have complex machined features that could make them open to failure from geometric stress conditions [4]. In general, more research and testing with piston configurations will allow General Fusion to find the right material and geometry for the system.

A final source of issue when it comes to this approach is the concept of cavitation, which takes place with the formation of vapor bubbles in the low pressure regions of a liquid that has been accelerated to high velocities (i.e. hit with a hammer/anvil piston coupling) [11]. On a macroscopic scale this distorts the flow pattern and could lead to non-uniformity, while on the microscopic scale this is transferred to pitting in the liquid lead interface. This was also found in the Mini-sphere project described in section II.C, where the wall vortex would turn into spray after the initial pressure wave propagation. This effect was thought to be a possible combination of RM instabilities and a cavitation region in the lead near the cavity due to the pressure rebound [4]. Work at General Fusion continues to simulate and optimize the error between piston firings in order to avoid these possible scenarios.

V. Final Remarks

To conclude, General Fusion's approach to viable fusion using established technologies enables a faster timeline and seems physically and economically feasible, but raises a few issues that are not present in more well-studied fusion reactor configurations. It remains to be seen if the issues present in Section IV (Challenges) of this paper only reduce the efficiency of the

reactor somewhat or pose greater problems, and more research is needed to comprehensively model the physics occurring within the reactor. As can be seen in the history of General Fusion's published literature, many alterations were made to the original reactor design - to date, the company has built at least a dozen prototypal plasma injectors and has experimented with various plasma configurations. Perhaps a different LMW material could mitigate the MHD effects of the liner upon compression, or a different distribution of steam pistons (or an entirely different source of compressive inertia) could prove helpful in countering the various mechanical instabilities present in the current design. If a successful reactor prototype is achieved, the compressed timeline of this company's reactor debut may shift the research paradigm of fusion energy away from the more established and researched MCF and ICF methods of achieving fusion. Such a reactor could bring more attention to MTF and the usage of inertial pistons as a viable way to achieve fusion energy in a way that could meet today's increasing energy demands.

References

- [1] V. Saponitsky, D. Plant, E. J. Avital, and A. Munjiza, “Propagation of Pressure Waves in Compression System Prototype for Magnetized Target Fusion Reactor in General Fusion Inc.,” in *30th International Symposium on Shock Waves 2*, Cham, 2017, pp. 955–960. doi: [10.1007/978-3-319-44866-4_30](https://doi.org/10.1007/978-3-319-44866-4_30).
- [2] W. J. Nuttall, S. Konishi, S. Takeda, and D. Webbe-Wood, Eds., *Commercialising Fusion Energy: How small businesses are transforming big science*. IOP Publishing, 2020. doi: [10.1088/978-0-7503-2719-0](https://doi.org/10.1088/978-0-7503-2719-0).
- [3] D. W. Kraft, “NUCLEAR FUSION BY MECHANICAL ADIABATIC COMPRESSION OF A DENSE PLASMA,” p. 8.
- [4] M. Laberge *et al.*, “Acoustically driven Magnetized Target Fusion,” in *2013 IEEE 25th Symposium on Fusion Engineering (SOFE)*, San Francisco, CA, USA, Jun. 2013, pp. 1–7. doi: [10.1109/SOFE.2013.6635495](https://doi.org/10.1109/SOFE.2013.6635495).
- [5] M. Reynolds, “Consequences of Flux Diffusion in a Liner Compression Fusion System,” p. 12.
- [6] R. Munipalli *et al.*, “Modeling Highly Unsteady Current-driven Liquid Metal Free-Surface MHD Flows,” p. 1.
- [7] A. Froese, D. Brennan, M. Reynolds, and M. Laberge, “MHD Stability of a Magnetized Target During Non-Self-Similar Compression,” p. 1.
- [8] K. Bol *et al.*, “Experiments on the Adiabatic Toroidal Compressor,” MATT--1092, IAEA-CN--33/A4-2, 4203067, Dec. 1974. doi: [10.2172/4203067](https://doi.org/10.2172/4203067).
- [9] P. O’Shea *et al.*, “Magnetized Target Fusion At General Fusion: An Overview,” p. 1.
- [10] D. Martelli, A. Venturini, and M. Utili, “Literature review of lead-lithium thermophysical properties,” *Fusion Engineering and Design*, vol. 138, pp. 183–195, Jan. 2019, doi: [10.1016/j.fusengdes.2018.11.028](https://doi.org/10.1016/j.fusengdes.2018.11.028).
- [11] “cavitation | physics | Britannica.” <https://www.britannica.com/science/cavitation> (accessed May 02, 2022).
- [12] A.A. Harms, K.F. Schoepf, and D.R. Kingdon. *Principles of Fusion Energy: An Introduction to Fusion Energy for Students of Science and Engineering*. World Scientific, 2000. isbn: 9789812380333. url: <https://books.google.com/books?id=DD0sZgutqowC>.
- [13] “Bringing fusion energy to market - fusion power,” General Fusion, 16-May-2022. [Online]. Available: <https://generalfusion.com/>. [Accessed: 16-May-2022].
- [14] “Conditions for fusion,” Lawson Criteria for Nuclear Fusion. [Online]. Available: <http://hyperphysics.phy-astr.gsu.edu/hbase/NucEne/lawson.html>. [Accessed: 16-May-2022].